ELSEVIER

Thin Solid Films 411 (2002) 106–114

thin solid films

www.elsevier.com/locate/tsf

Defect chemistry and physical properties of transparent conducting oxides in the CdO-In_2O_3-SnO_2 system

T.O. Mason[a,*], G.B. Gonzalez[a], D.R. Kammler[b], N. Mansourian-Hadavi[a], B.J. Ingram[a]

[a]*Northwestern University, Department of Materials Science and Engineering and Materials Research Center, 2225 North Campus Drive, Evanston, IL 60208, USA*

[b]*Sandia National Laboratories, Albuquerque, NM 87185, USA*

Abstract

Combined solid state phase diagram studies and physical property measurements of the various n-type transparent conducting oxide (TCO) phases in the CdO-In_2O_3-SnO_2 system have been carried out. The 1175 °C (air) subsolidus phase diagram has been established, including solid solution limits for binary and ternary compositions. From these limits and electrical property measurements vs. doping and degree of reduction, the prevailing defect mechanisms can be deduced. In addition to intrinsic (native) defects (e.g. oxygen vacancies) and extrinsic donor-doping of the end member compounds (e.g. $Sn^{\bullet}_{In}$ in In_2O_3), ternary solid solutions exhibit both isovalent doping (e.g. $[Cd'_{In}]=[Sn^{\bullet}_{In}]$ in bixbyite, spinel) and donor-to-acceptor imbalance (e.g. $[Sn^{\bullet}_{In}]>[Cd'_{In}]$ in bixbyite, spinel). Aliovalent doping can also lead to the formation of point defect associates, as in Sn-doped In_2O_3 (ITO), as confirmed by combined Rietveld analyses of X-ray and neutron diffraction data. Cation exchange between sublattices in the spinel phase plays an important role in determining phase stability and band structure. The physical properties of the TCO phases in the CdO-In_2O_3-SnO_2 system are presented for both bulk ceramics and thin films.

Keywords: Transparent conducting oxides; Phase diagram; Point defects; Electrical properties; Optical properties

1. Introduction

The defect structures of oxides based upon CdO, In_2O_3, and/or SnO_2 play a major role in determining their unique electrical and optical properties, which qualify them to serve as transparent conductors in a variety of well-known applications. Each of these constituent oxides, the more complex binary compounds they form, and the binary/ternary solid solutions based upon them prove to be n-type, so we will restrict our attention almost exclusively to donor-doping mechanisms. Both extrinsic and intrinsic doping can be used to generate carriers. Widely recognized examples of extrinsic doping include Sn-doping of In_2O_3 (so-called ITO) and Sb-doping of SnO_2. The latter instance involves dopant species outside the CdO-In_2O_3-SnO_2 system, and will therefore not be considered in the present study. Virtually all n-type TCO materials undergo some form of intermediate temperature reduction to enhance the electron population. It has been postulated that such a reduction increases native (intrinsic) defects such as oxygen vacancies, which act as donor species alongside any extrinsic species that may be present. Point defects not only set the carrier concentrations in TCOs, but they also influence carrier mobility due to ionized and neutral impurity scattering. Our focus is primarily on carrier generation; a discussion of scattering mechanisms in TCOs is found elsewhere [1].

The present study provides a review of literature results and recent work in our laboratory concerning the CdO-In_2O_3-SnO_2 system. Virtually all of this work has already appeared in print, so experimental details will be limited to what is necessary to interpret the research findings and their implications insofar as defect models are concerned.

Beginning with an overview of the recently established CdO-In_2O_3-SnO_2 subsolidus phase diagram (at 1175 °C in air) and the phases present [2,3], defect models are considered for the undoped end-members, the binary solid solutions they form (including a discussion of point defect associates in ITO), and finally the

*Corresponding author. Tel.: +1-847-491-3198; fax +1-847-491-7820.

E-mail address: t-mason@northwestern.edu (T.O. Mason).

0040-6090/02/$ - see front matter
PII: S0040-6090(02)00197-9

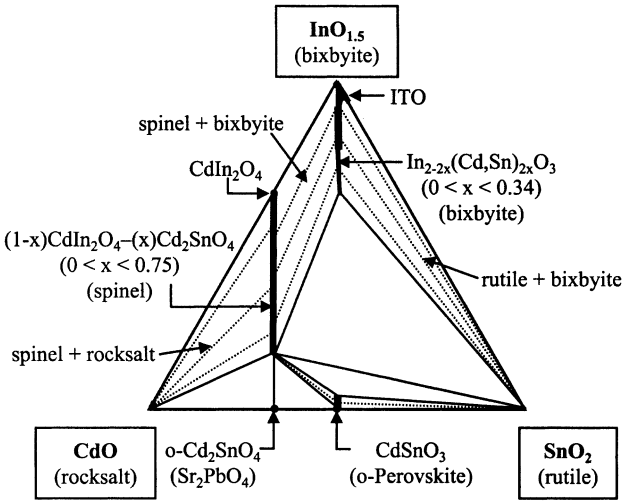

Fig. 1. Subsolidus phase relations in the CdO-$InO_{1.5}$-SnO_2 system at 1175 °C adapted from [2].

binary compounds which form and their solid solution ranges—both binary and ternary. In every case, the phase diagram provides essential information regarding doping mechanisms in these materials. This solubility information can be combined with electrical property studies to elucidate the probable point defect mechanisms. The paper concludes with a comparison of bulk and thin film electrical and optical properties of the TCO phases in the CdO-In_2O_3-SnO_2 system.

2. The CdO-In_2O_3-SnO_2 phase diagram

The standard solid state reaction method was employed to investigate subsolidus phase relations at 1175 °C in the CdO-In_2O_3-SnO_2 system, as outlined elsewhere [23]. Pressed compacts of high purity component oxides (>99.99% pure) were reacted in an alumina crucible inside a bed of sacrificial powder (of the same composition) with a tightly fitting cover to limit Cd volatilization. Repeated firing and regrinding steps were required to reach equilibrium, as determined by X-ray diffraction. In addition to identifying the phases present, peak positions (corrected for off-axis displacement and zero-shift errors with an internal Si standard) were used to calculate lattice constants and establish solubility limits by Vegard's law. In several cases, intentionally biphasic assemblages were prepared to saturate a majority TCO phase with a small amount of second phase. This allowed for the lattice parameter(s) of the terminal TCO composition to be established, and its electrical properties were measured (see below).

The resulting phase diagram is displayed in Fig. 1. The stoichiometry of the In_2O_3 end-member is written as $InO_{1.5}$ so that the ratio of component oxides corresponds to the Cd:In:Sn ratio in all phases. No binary compounds were obtained in the $InO_{1.5}$-SnO_2 binary, in agreement with previous work [4,5]. A single binary compound, having the spinel structure and stoichiometry ($CdIn_2O_4$), was obtained in the CdO-$InO_{1.5}$ binary, in agreement with Morozova and Komarov [6]. In the CdO-SnO_2 binary, two phases were observed, both exhibiting orthorhombic symmetry—$CdSnO_3$, with the $GdFeO_3$ distorted perovskite structure, and Cd_2SnO_4, with the Sr_2PbO_4 structure—in agreement with the early work of Smith [7]. Binary solubility limits, as shown on the diagram, will be discussed further below. Although no ternary compounds were found, three relatively extensive ternary solid solution ranges were identified. At the top of the diagram, bixbyite In_2O_3, which dissolves limited SnO_2 and negligible CdO, dissolves up to 34 cation percent of Sn and Cd for In, as expressed by the formula, $In_{2-2x}(Cd,Sn)_{2x}O_3$ $(0 \le x < 0.34)$. Similarly, the $CdIn_2O_4$ spinel phase dissolves up to 75 cation percent of Sn and Cd for In, as expressed by the formula, $Cd_{1+x}In_{2-2x}Sn_xO_4$ $(0 \le x < 0.75)$. Another way to consider the spinel solid solution is as extending 75 percent of the way from $CdIn_2O_4$ to Cd_2SnO_4, i.e. $(1-x)CdIn_2O_4-(x)Cd_2SnO_4$, with allowed values of x ranging from 0 to 0.75. It is interesting to note that while Cd_2SnO_4 spinel can be readily produced in thin film form [8–10], it is unstable as a bulk phase (at 1175 °C). Finally, the orthorhombic $CdSnO_3$ phase was shown to substitute up to 4.5 cation% of In for each of Cd and Sn, i.e. $(Cd,Sn)_{1-x}In_{2x}O_3$ $(0 \le x < 0.045)$.

3. The defect chemistry of the end member oxides (CdO, In_2O_3, SnO_2)

3.1. Intrinsic point defects

There appears to be general consensus in the literature that the prevailing native point defect mechanism in each of the end-member oxides is the formation of oxygen vacancies [11–18]:

$$O_O^x \Leftrightarrow 1/2O_2(g) + V_O^{\bullet\bullet} + 2e' \quad (1)$$

where species are written in standard Kröger–Vink notation. This conclusion is largely based on equilibrium electrical property measurements, which exhibit a $pO_2^{-1/6}$ dependence in accordance with Eq. (1). In the case of In_2O_3, oxygen deficiency was confirmed by high temperature TGA studies [17]. In the case of CdO, the alternative native donor reaction:

$$Cd_{Cd}^x + O_O^x \Leftrightarrow 1/2O_2(g) + Cd_i^{\bullet\bullet} + 2e' \quad (2)$$

cannot be ruled out based upon the electrical properties, since an identical pO_2 dependence ($pO_2^{-1/6}$) is predicted for electrons. (It should be noted that this is not an issue for In_2O_3 or SnO_2, since their corresponding interstitial formation reactions yield noticeably different

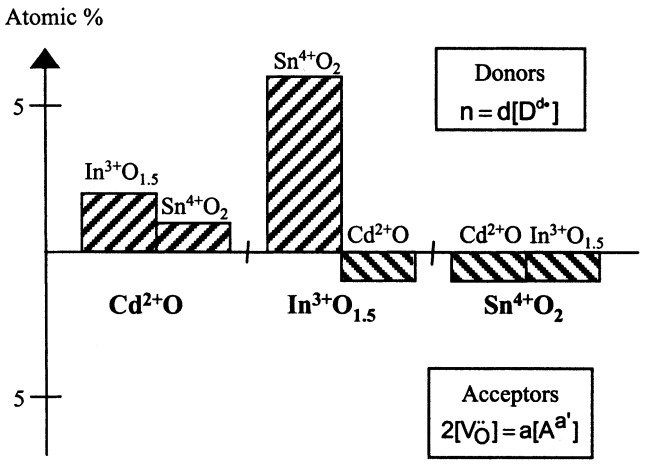

Fig. 2. Solid solution solubility limits of the binary solid solutions based on the end members of the CdO-$InO_{1.5}$-SnO_2 system.

pO_2 dependences.) Straumanis et al. [12] argued convincingly for oxygen vacancies over cadmium interstitials in CdO, based on decreasing density with decreasing pO_2. Furthermore, cation interstitials have not been reported in rocksalt oxides, most likely due to ionic size limitations; the only exception is FeO, where iron interstitials exist only in combination with vacancies in extended point defect clusters [19]. It is therefore likely that the oxygen vacancy reaction dominates the defect chemistry of each of the undoped end-members in the CdO-In_2O_3-SnO_2 system.

3.2. Extrinsic doping of the end members (binary solid solutions)

In Fig. 2, the six binary solid solutions of the CdO-In_2O_3-SnO_2 system are examined. Donor doping is represented in the upper portion of Fig. 2, whereas acceptor doping is represented in the lower portion. The assignment of these solubility limits was predicated on the basis of combined electrical property and X-ray diffraction studies.

To track the generation of charge carriers with doping, room temperature conductivity was measured by four-probe apparatus (Cascade Microtech, Beaverton, OR) on pellets pressed and sintered as described above. Correction factors were applied to account for the finite sample dimensions [20], but the results were not corrected for sample porosity. Similarly, Seebeck coefficients were measured by placing the sample pellets between a 24 W heater and a cold sink (with intervening gold foil contacts to which type-S thermocouples were attached). After an initial heating surge and a period of thermal relaxation, thermovoltage and temperature differences were made near 60 °C with gradients of 20 °C or less. Seebeck coefficients (α) were corrected for the thermopower of platinum.

The lower portion of Fig. 2 represents acceptor-doping situations, i.e. Cd'_{In} in In_2O_3, and either Cd''_{Sn} or In'_{Sn} in SnO_2. In no instance, however, was p-type character observed. Instead, the otherwise relatively conductive n-type parent oxides were rendered insulating; their conductivities were lower than could be measured in our four probe apparatus (<0.01 S/cm). This is to be expected, however, based upon the oxygen vacancy reaction of Eq. (1). Such acceptors can be ionically compensated by oxygen vacancies, e.g. $[Cd'_{In}]=2[V_O^{\cdot\cdot}]$ in In_2O_3 and $[In'_{Sn}]=2[V_O^{\cdot\cdot}]$ or $[Cd''_{Sn}]=[V_O^{\cdot\cdot}]$ in SnO_2. For example, CdO-doping of In_2O_3 takes place according to:

$$2CdO \Rightarrow 2Cd'_{In} + 2O_O^x + V_O^{\cdot\cdot} \quad (3)$$

(The forward arrow indicates that this reaction goes to completion during synthesis.) As the oxygen vacancy concentration increases, the electron population must decrease according to Eq. (1), leading to decreased conductivities. The lack of an electronic compensation mechanism for acceptors (i.e. holes) also accounts for the relatively limited solubilities in each of these situations. Although there is a detectable increase in the lattice parameter of In_2O_3 upon CdO-doping, the terminal solubility was estimated to be on the order of 1 cation% [3,21], in agreement with Morozova and Komarov [6]. In contrast, there was no detectable change in the unit cell volume of SnO_2 in the presence of a small excess of either o-$CdSnO_3$ or In_2O_3. The fact that these biphasic specimens were too resistive for reliable electrical measurements suggests that some degree of acceptor doping has been achieved. Neither Edwards and Mason (1250 °C) [4] nor Bates et al. (1527–1577 °C) [5] could detect significant In-solubility in SnO_2. Likewise, Smith [7] reported negligible solubility of In_2O_3 in SnO_2 between 1000 and 1100 °C. The solubility limits shown in Fig. 2 for SnO_2 of 1 cation% are generous; actual solubilities are probably much smaller. It must be stressed that this does not indicate SnO_2 to be a poor TCO, rather that suitable donor species (with higher valence states, such as Sb^{5+}) do not exist in the CdO-In_2O_3-SnO_2 system.

On the other hand, the upper portion of the chart in Fig. 2 corresponds to donor doping situations—$In_{Cd}^{\cdot}$ or $Sn_{Cd}^{\cdot\cdot}$ in CdO and $Sn_{In}^{\cdot}$ in In_2O_3. For example, SnO_2-doping of In_2O_3 can proceed according to:

$$2SnO_2 \Rightarrow 2Sn_{In}^{\cdot} + 3O_O^x + 2e' + {}^1/_2O_2(g) \quad (4)$$

Again, the forward arrow indicates this reaction goes to completion during synthesis. Up to 6 cation% Sn was found to be soluble in In_2O_3, in agreement with Edwards and Mason [4]; the resulting materials were conductive, with high electron populations. Somewhat higher solubility limits have been reported in bulk studies [22], with up to 22 cation% being reported in thin films [23].

The solubilities of In_2O_3 and SnO_2 in CdO are considerably smaller than SnO_2 in In_2O_3, as shown in Fig. 2. In neither case could a change in CdO lattice parameter be detected. Nevertheless, the magnitude of the Seebeck coefficient decreased significantly (increased electron population) from pure CdO to 1 cation% Sn and out to 2 cation% In, resulting in comparable levels (-10 to -15 $\mu V/K$), but appeared to be constant at higher doping levels (with second phases present). A minor amount of second phase was present at the 1% Sn doping level (o-Cd_2SnO_4), but not at the 2% In doping level by XRD. Based upon anticipated lattice parameter vs. composition behavior and experimental XRD uncertainties, the solubility limit of In in CdO should be less than 3 cation% [3]. Fig. 2 shows 1 cation% and 2 cation% limits for Sn and In, respectively. As in the case of Sn-doped In_2O_3, significantly higher solubility limits have been reported in thin films for both In-doped CdO [24] and Sn-doped CdO [25].

The results summarized in Fig. 2 indicate that the end-member compounds can be extrinsically donor-doped to a substantial extent (e.g. Eq. (6)), however, acceptor-doping is limited and results in ionic compensation (by oxygen vacancies, Eq. (5)) instead of electronic compensation (by holes). This is not the entire story, however, since point defect associates must also be considered.

3.3. Defect associates in Sn-doped In_2O_3

Indium oxide crystallizes in the cubic C-type rare-earth sesquioxide structure, otherwise referred to as bixbyite. This structure can be derived from the related fluorite structure by removing one fourth of the anions, and allowing for small shifts of the ions. Indium cations reside at two non-equivalent six-fold positions, referred to as equipoints 'b' and 'd', according to international notation (see Fig. 3). The b-site cations are bounded by two structural vacancies along a body-diagonal as shown. The d-site cations are bounded by two structural vacancies along a face-diagonal as shown. It should be stressed that these structural vacancies are actually empty oxygen interstitial positions.

Bixbyite is quite unique in this regard; close-packed structures such as rocksalt and spinel lack such empty anion interstitial positions.

Unusual carrier content vs. doping and vs. pO_2 behavior was reported in ITO films by Frank and Kostlin [23]. In particular, carrier content saturated and remained relatively unchanged beyond a specific Sn-doping level. Also, a $pO_2^{-1/8}$ dependence of electrical properties (at fixed Sn content) was observed in films and in later equilibrium bulk studies [26], which cannot be explained on the basis of Eq. (1). Frank and Kostlin [23] proposed the existence of neutral $(2Sn_{In}^{\bullet}O''_i)^x$ associates, which

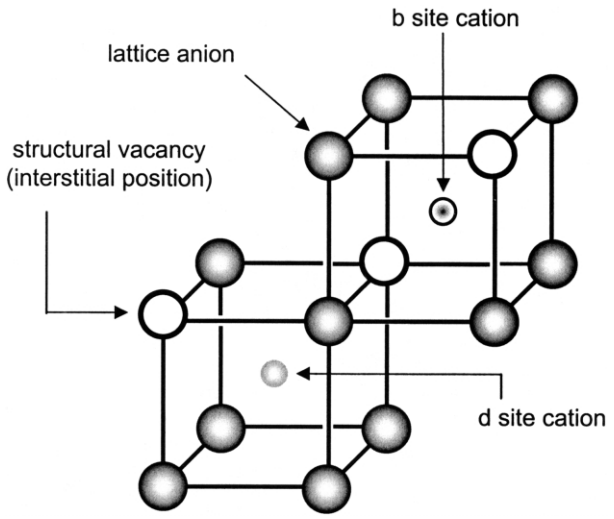

Fig. 3. Schematic representation of the b and d cation sites in the bixbyite structure adapted from [27].

can form in the doping of In_2O_3 (during synthesis):

$$2SnO_2 \Rightarrow (2Sn_{In}^{\bullet}O''_i)^x + 3O_O^x \quad (5)$$

and yet be subsequently reduced at lower temperatures to remove the oxygen interstitials, thereby increasing the number of free Sn-donors:

$$(2Sn_{In}^{\bullet}O''_i)^x \Leftrightarrow {}^1/_2O_2(g) + 2Sn_{In}^{\bullet} + 2e' \quad (6)$$

At high doping levels and under oxidizing conditions, most of the Sn is bound up in associates. This explains why the electron population changes negligibly beyond a certain overall Sn-level; added Sn beyond this point incorporates as neutral associates and does not affect the electroneutrality condition. This model also accounts for the observed $pO_2^{-1/8}$ dependence at a fixed overall Sn-level, which follows from Eq. (6) if the concentration of $(2Sn_{In}^{\bullet}O''_i)^x$ is assumed to be invariant.

To establish the existence of $(2Sn_{In}^{\bullet}O''_i)^x$ associates in ITO, we carried out time-of-flight neutron diffraction experiments on undoped and 4.5 cation% doped ITO, sintered at 1350 °C, subsequently equilibrated at 800 °C under oxidizing (air) or reducing (CO/CO_2) conditions, and quenched. This work was performed at the Intense Pulsed Neutron Source at Argonne National Laboratory. Details concerning sample preparation and indium absorption corrections are given elsewhere [27]. Rietveld analysis confirmed the absence of oxygen interstitials in undoped In_2O_3 and the existence of oxygen interstitials in ITO. Furthermore, the ratio of Sn-to-oxygen interstitials in ITO was 2.2 ± 0.3, which is consistent with the $(2Sn_{In}^{\bullet}O''_i)^x$ associate. As predicted by Eq. (6), the interstitial population was much smaller in the reduced specimen (the Sn-to-oxygen interstitial ratio increased to 6.2 ± 2.2), but it was not zero. Frank and Kostlin made similar observations and proposed the existence

of more complex 'non-reducible' associates to discriminate them from the reducible $(2Sn^{\bullet}_{In}O''_i)^x$ species [23].

It is likely that $(2Sn^{\bullet}_{In}O''_i)^x$ associates play a more decisive role in the defect chemistry of ITO than do intrinsic defects (i.e. oxygen vacancies, Eq. (1)). These associates may be responsible for the high concentrations of Sn, which can be incorporated in ITO. Doping by neutral associates (Eq. (5)) appears to be energetically favored over doping by isolated donors (Eq. (4)). Although there is no evidence that isolated oxygen interstitials are ever majority defects in ITO (they would serve as acceptors), the numerous 'structural vacancies' in the bixbyite structure do allow for their existence, but only in local combination with Sn-donor species. Once incorporated, the excess Sn tied up in neutral associates serves as a reservoir for the production of additional free Sn-donors upon removal of oxygen interstitials during reduction (Eq. (6)). Although some oxygen vacancy donors are undoubtedly produced during the reduction step (Eq. (1)), the removal of oxygen interstitials from associates (Eq. (6)) probably dominates the reduction process insofar as carrier production is concerned.

A similar pO_2-dependence of electrical properties ($pO_2^{-1/8}$) was recently observed in a related TCO phase, GITO or $Ga_{3-x}In_{5+x}Sn_2O_{16}$ $(0.3<x<1.6)$, and was interpreted in terms of the same associate model [26]. However, the excess Sn content (extra Sn on In sites) was found to be much smaller ($[Sn^{\bullet}_{In}]<1\%$). This may be because GITO has only body-diagonal cation sites as opposed to both body-diagonal and face-diagonal sites in ITO. Current work is aimed at assessing the roles of 'b' vs. 'd' sites (and their combination) in stabilizing the formation of associates in ITO.

4. The defect chemistry of ternary solid solutions

4.1. Isovalent substitutions

As pointed out previously, ternary solid solutions in the CdO-In_2O_3-SnO_2 system are considerably more extensive than their binary counterparts. It is also apparent that these tend to occur at a constant Cd-to-Sn ratio, i.e. they appear as vertical lines in the phase diagram of Fig. 1. This is due to the fact that the substitutions in question are largely isovalent. For example, in bixbyite co-doped with Cd and Sn, two In^{3+} species are replaced by one Cd^{2+} and one Sn^{4+} with no net change in overall charge balance. In Kröger–Vink notation, the synthesis reaction can be represented as:

$$CdO + SnO_2 \Rightarrow Cd'_{In} + Sn^{\bullet}_{In} + 3O^x_O \quad (7)$$

such that $[Cd'_{In}] = [Sn^{\bullet}_{In}]$. The reverse process takes place in o-$CdSnO_3$, where one Cd^{2+} and one Sn^{4+} are replaced by two In^{3+} species, again with no net change in the overall charge balance:

$$In_2O_3 \Rightarrow In^{\bullet}_{Cd} + In'_{Sn} + 3O^x_O \quad (8)$$

such that $[In^{\bullet}_{Cd}] = [In'_{Sn}]$.

The situation in the $CdIn_2O_4$-Cd_2SnO_4 spinel solid solution is complicated by the possibility of cation exchange between tetrahedral and octahedral sublattices (see below). However, if for the moment we assume $CdIn_2O_4$ to have a 'normal' distribution and Cd_2SnO_4 to have an 'inverse' distribution (not far from the actual situation—see below), the solid solution can be expressed as:

$$(Cd)^{tet}(In_{2-2x}Cd_xSn_x)^{oct}O_4 \quad (9)$$

where the first set of parentheses encloses the tetrahedral species (exclusively Cd) and the second set encloses the octahedral species. The replacement process (octahedral site) can be expressed as:

$$CdO + SnO_2 + 2In^x_{In} \Rightarrow In_2O_3 + Cd'_{In} + Sn^{\bullet}_{In} \quad (10)$$

such that $[Cd'_{In}] = [Sn^{\bullet}_{In}]$. The fact that co-substitution is isovalent in this case, as in the two previous cases, is largely responsible for the extended solid solubility range allowed. It is also true that the average of the Cd^{2+} and Sn^{4+} cation radii (in octahedral co-ordination) is very close to that of In^{3+} according to Shannon [28].

The problem, however, with strictly isovalent co-substitutions is that they should have no influence on the electroneutrality condition. Neglecting native defects for the moment, this means that any composition falling precisely on the vertical (cation-stoichiometric) lines of Fig. 1 ought to be insulating. This is never observed in any of the ternary solid solution phases—bixbyite, spinel, or o-$CdSnoO_3$. It is therefore proposed that inherent imbalance of donor vs. acceptor species is responsible for the n-type behavior of these phases.

4.2. Donor vs. acceptor imbalance in co-substituted phases

Intentionally 2% CdO-rich and 2% SnO_2-rich compositions were prepared at 5 cation% increments along the bixbyite line of stoichiometry in Fig. 1, i.e. to either side of the line such that the major phase (bixbyite) was saturated with second phase spinel or rutile (SnO_2), respectively [21]. The amount of the second phase, however, was limited in order to minimize its effect on the composite conductivity. The room temperature conductivities of the CdO-rich specimens were comparable to those of as-fired materials of nominal composition, $In_{2-2x}Cd_xSn_xO_3$. Furthermore, the ratio of conductivity of a SnO_2-rich sample to that of the corresponding CdO-rich sample was relatively small, decreasing from ~ 30 (at nominal $x=0.05$) to essentially unity (at nominal $x=0.34$). This is indicative of a limited phase field width for bixbyite, which decreases with increasing x. More importantly, however, is the observation that even bixbyite saturated with excess spinel (CdO-rich) main-

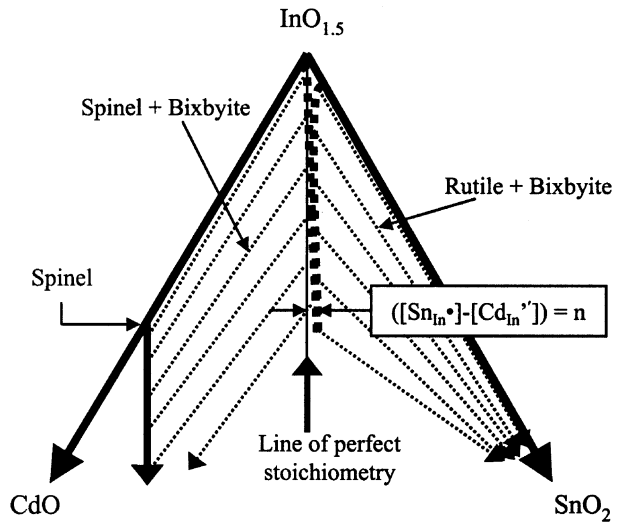

Fig. 4. Proposed bixbyite phase field in the CdO-$InO_{1.5}$-SnO_4 system adapted from [21].

tains n-type character, with conductivities not significantly smaller than for SnO_2-rich compositions. Furthermore, nominal solution compositions with large values of x ($x \rightarrow 0.34$) exhibit small or negligible increases in conductivity upon reduction for 6 h in 4% H_2, 96% N_2 at 400 °C. We have interpreted these findings in terms of an inherent donor-to-acceptor imbalance, i.e. $[Sn^{\bullet}_{In}] > [Cd'_{In}]$, such that (with increasing x) the electroneutrality condition is increasingly dominated by:

$$n = \left\{[Sn^{\bullet}_{In}] - [Cd'_{In}]\right\} \quad (11)$$

It is possible that this cation non-stoichiometry is established kinetically during synthesis by preferential Cd volatilization. However, this does not explain the behavior of CdO-rich samples, in which the second phase serves as a reservoir for CdO. It is more likely that the equilibrium phase field of bixbyite deviates from the line of perfect stoichiometry, as shown in Fig. 4. With increasing co-substitution (x), the phase field width decreases (decreasing the ratio of rutile-saturated to spinel-saturated conductivities) and its position shifts to the right from perfect stoichiometry (enhancing the donor-to-acceptor imbalance of Eq. (11), thereby reducing the sensitivity of electrical properties to reduction).

A similar donor-to-acceptor imbalance has been proposed for the spinel solid solution [3,29]. As discussed previously, stoichiometric $CdIn_2O_4$, Cd_2SnO_4, and their solid solution should be insulating, since they are completely charge-balanced. As described above, co-substitution as per Eq. (10) results in a balance of donors and acceptors, $[Cd'_{In}] = [Sn^{\bullet}_{In}]$. We took advantage of the preferential volatilization of Cd to perform the following experiment. A specimen with nominal composition, [Cd] = 60, [In] = 25, [Sn] = 15, was allowed to pre-equilibrate to a mixture of CdO and spinel (two-phase assemblage in Fig. 1). Electrodes were attached to a bar of this material, and electrical conductivity was monitored vs. time under flowing air at 1090 °C. This allowed for relatively rapid cadmium loss due to volatilization, with a resulting composition path that crossed the spinel line in Fig. 1 at approximately $x = 0.5$ in $(1-x)CdIn_2O_4 - (x)Cd_2SnO_4$, before ultimately entering the two-phase (spinel + bixbyite) region. Parallel XRD experiments were performed on identically prepared specimens, which were periodically removed from the furnace, quenched to room temperature, and analyzed for phases present. The spinel conductivity rose gradually from a relatively high value with excess CdO present to a value only 30% higher with excess bixbyite present. This indicates that there is some width to the spinel phase field, but more importantly, even CdO-saturated spinel is highly donor-doped.

It may be argued that intrinsic defects (e.g. oxygen vacancies, Eq. (1) or cadmium interstitials, Eq. (2)) are responsible for the inherent n-type character of the spinel phase. However, this is not supported by reduction experiments on bulk specimens (6 h in 4% H_2, 96% N_2 at 400 °C), where rather insignificant increases over as-fired values were obtained (typically only 20–30%) [29]. This supports our contention that donor vs. acceptor imbalance (e.g. Eq. (11)) is the prevailing source of electrons. On the other hand, supplemental cadmium interstitial donors are possible. As opposed to the close-packed rocksalt structure, which does not readily accommodate cation interstitials, there are copious cation interstices in the spinel structure, where only 1/8 of the tetrahedral positions and half of the octahedral positions are normally occupied. Cd_2SnO_4 films are routinely annealed in the presence of CdS. The resulting cadmium vapor can provide additional donors according to:

$$Cd(g) \Rightarrow Cd^{\bullet\bullet}_{i} + 2e' \quad (12)$$

thereby adding to the electrons present due to cation non-stoichiometry.

An excess of donors over acceptors in $CdIn_2O_4$ ($[In^{\bullet}_{Cd}] > [Cd'_{In}]$) or in Cd_2SnO_4 ($[Sn^{\bullet\bullet}_{Cd}] > [Cd''_{Sn}]$) requires that the spinel phase field lie slightly to the right of the line of perfect stoichiometry in Fig. 1. Mulligan [30] and Kammler et al. [3,29] observed systematic shifts away from nominal (target) composition in RF-sputtered films that would support this interpretation. Wei and Zhang [31], using a first-principles band-structure method, determined the relative energetics for Sn-on-Cd antisite defects vs. oxygen vacancies in Cd_2SnO_4 spinel. They concluded that the antisite species, which were energetically favored over oxygen vacancies, were responsible for the prevailing n-type character of cadmium stannate.

4.3. The role of cation distribution in the spinel phase

There is one last point defect reaction that is unique to the spinel structure. This involves the exchange of cations between tetrahedral and octahedral sites. For example, the inversion of the cation distribution in 'normal' $CdIn_2O_4$ can be described by:

$$\begin{matrix}(1-\lambda)\ (2-\lambda) & (\lambda) & (\lambda)\\ Cd^{x}_{Cd}+In^{x}_{In} & \Leftrightarrow Cd'_{In}+In^{\bullet}_{Cd}\end{matrix} \qquad (13)$$

where λ is the inversion parameter. When $\lambda=0$, the distribution is completely normal (all Cd is on tetrahedral sites and all In is on octahedral sites); when $\lambda=1$, the distribution is inverse (all Cd on octahedral sites and the In cations are divided evenly between tetrahedral and octahedral sites). Note that this redistribution is charge-balanced and does not affect the electroneutrality condition, i.e. $[Cd'_{In}]=[In^{\bullet}_{Cd}]=\lambda$.

We conducted a combined TEM-ALCHEMI (atom location by channeling-enhanced microanalysis) [32],^{119}Sn Mössbauer [33], and neutron/X-ray diffraction study [33] of the cation distribution in $(1-x)CdIn_2O_4-(x)Cd_2SnO_4$. Special ^{112}Cd-enriched bulk samples were prepared at $x=0$ and $x=0.7$ to avoid the unacceptably large neutron absorption cross-section of the ^{113}Cd isotope (12% of naturally occurring Cd). The distribution obtained for bulk specimens quenched from 1175 °C is shown in Fig. 5a. (The solid lines were obtained using the thermodynamic model of O'Neill and Navrotsky [34].) Mössbauer results indicate that the Sn resides exclusively on octahedral sites (i.e. Cd_2SnO_4 is an inverse spinel [35]). However, the degree of inversion for $CdIn_2O_4$ was found to be significant at 1175 °C ($\lambda\sim0.31$). This may play an important role in determining the stability range of the spinel phase. As $CdIn_2O_4$ is doped with Cd_2SnO_4, the co-substitution process of Eq. (10) (Cd and Sn for two In) takes place almost exclusively on the octahedral sublattice. By $x=0.7$, however, the octahedral Cd concentration saturates (~1) and Cd begins to replace the residual In on tetrahedral sites. It is just beyond this point that the spinel structure becomes no longer stable (in bulk materials).

At much lower temperatures, where films are produced, the cation distribution should approach the ideal distribution represented in Fig. 5b (normal $CdIn_2O_4$ to inverse Cd_2SnO_4). In this case, octahedral co-substitution (Cd and Sn for two In) is possible all the way to Cd_2SnO_4. This may explain why spinel cadmium stannate, which is unstable in bulk form, can be readily prepared in thin film form, however, the state of strain in thin films may also play a role [3].

The cation distribution may also play an important role in establishing the fundamental band gap. Wei and Zhang predicted by first principles band structure calculations that normal $CdIn_2O_4$ (predicted to be the stable form) should have a fundamental band gap 1.07 eV larger than for inverse $CdIn_2O_4$ [36]. This suggests that the fundamental band gap can be 'engineered' by altering the inversion parameter of Eq. (13) through adjustment of quench temperature and/or composition, independently of any Burstein–Moss shifts resulting from doping. This method of control appears to be unique to the spinel TCOs.

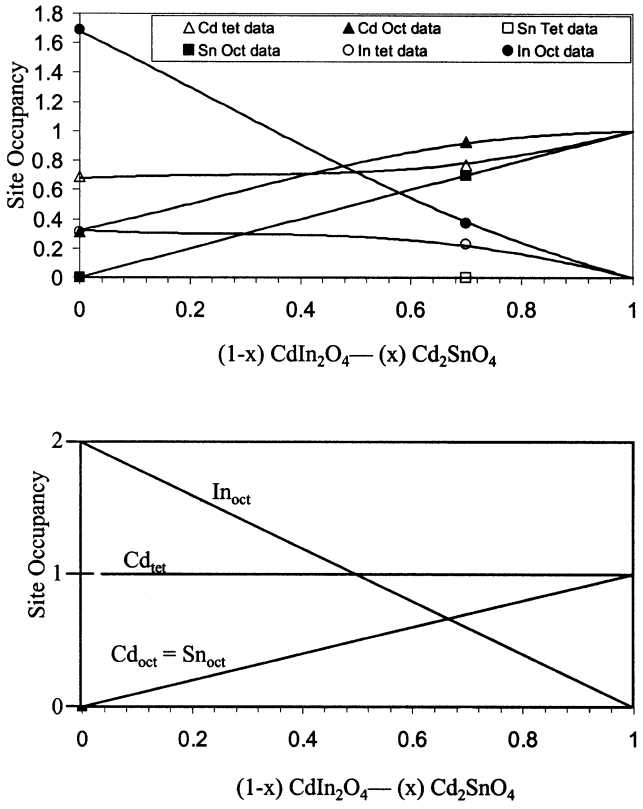

Fig. 5. Cation site distributions in $(1-x)\ CdIn_2O_4-(x)\ Cd_2SnO_4$ (after [33]). (a) Samples quenched from 1175 °C (solid lines determined from [34]) and (b) fully relaxed (normal $CdIn_2O_4$-to-inverse Cd_2SnO_4 cation distribution.

5. Physical properties of bulk and thin film phases

Tables 1 and 2 catalogue the electrical and optical properties of bulk and thin film TCO phases in the CdO-In_2O_3-SnO_2 system. Most of the thin film data were drawn from various literature sources, as indicated. It should be stressed that the bulk conductivity results were made on porous samples ($\sim$60% dense) and were not corrected for porosity; true conductivities will be much larger [2,3]. Nevertheless, these raw data allow for screening and meaningful comparisons between phases in the system. Optical gaps were obtained by diffuse reflectance measurements of the bulk materials, and by absorption measurements on thin films.

Table 1
Bulk specimen property summary data table [2,3]

Phase	Conductivity (S/cm)		Thermopower (μV/K)		Optical gap (eV)	
	As fired	Reduced	As fired	Reduced	As fired	Reduced
ITO [38] ($In_{1.92}Sn_{0.08}O_3$)	919	1270			3.3	
Ternary bixbyite ($x=0.25$)	290	420	−34	−29	3	3.1
$CdIn_2O_4$	550	650		−51	2.8	2.8
Cd_2SnO_4 (orthorhombic)	760	910	−81		2.6	2.6
Ternary spinel ($x=0.70$)	1450	2000		−35	2.8	2.8
$Cd_{1-x}Sn_{1-x}In_{2x}O_3$[a]	200		−60		3.1	

In the case of solid solutions, the properties of the best composition are listed.
[a] This specimen had a small amount of spinel and rutile secondary phases.

Table 2
Thin-film specimen property summary data table

Phase	Conductivity (S/cm)	Mobility (cm^2/Vs)	Carrier density (l/cm^3)	Optical gap (eV)
ITO[a]	5000–10 000	41	7.5×10^{20}	–
$CdIn_2O_4$ [10][b]	4300	44	6.1×10^{20}	–
Cd_2SnO_4 [10][b]	8300	60	9.0×10^{20}	3.7 [27]
Ternary spinel ($x=0.70$)[b]	4000	56	4.9×10^{20}	3.7
CdO [22]	3600	146	1.5×10^{20}	2.8
$Cd_{1-x}Sn_xO$ [25][c]	42 000	609	4.74×10^{20}	2.78
$Cd_{1-x}In_xO$ ($x=0.05$) [24]	16 800	69	1.5×10^{21}	3.1

[a] Typical values, i.e. see [39].
[b] Films treated in Ar/CdS.
[c] Films grown epitaxially on MgO.

Table 3
Donor-doping mechanisms, ionic compensation mechanisms, and antisite disorder in the $CdO\text{-}In_2O_3\text{-}SnO_2$ system

Donor doping	*Phases*
$n=2[V_O^{\bullet\bullet}]$	CdO, In_2O_3, SnO_2, (all)
$n=2[D^{d\bullet}]$	CdO:In, CdO:Sn, In_2O_3:Sn
$n=(d[D^{d\bullet}]-a[A^{a'}])$	Co-doped bixbyite, spinel, o-$CdSnO_3$
$\Delta n=2[Cd_i^{\bullet}]$	spinel
Ionic compensation	*Phases*
$2[V_O^{\bullet\bullet}]=[A^{a'}]$	In_2O_3:Cd, SnO_2:Cd, SnO_2:In
$[Cd'_{In}]=[Sn_{In}^{\bullet}]$	Co-doped bixbyite, spinel
$[In'_{Sn}]=[In_{Cd}^{\bullet}]$	o-$CdSnO_3$:In
$(2Sn_{In}^{\bullet}O''_i)^x$	In_2O_3:Sn
Antisite disorder	*Phases*
$(Cd_{1-\lambda}In_\lambda)(In_{2-\lambda}Cd_\lambda)O_4$	spinel

All known phases in the $CdO\text{-}In_2O_3\text{-}SnO_2$ system are good-to-excellent n-type transparent conductors. SnO_2 is not included in the tables, due to the fact that it is not an acceptor-doped material in this system. However, it is well known that SnO_2 can be rendered conducting by suitable donor-doping (e.g. by $Sb_{Sn}^{\bullet}$ or $F_O^{\bullet}$) and is actually the most used commercial TCO [37]. Otherwise, the best conductors are ITO and the spinel phase (especially with increasing Cd_2SnO_4 content), based upon bulk properties. This is borne out in the thin film data. The most promising behavior, however, is that of CdO. Undoped films of CdO have conductivities rivaling that of Sn-doped In_2O_3 (ITO). With extrinsic doping (by In or Sn), extremely high conductivities (and mobilities) can be achieved, with corresponding increase of the band gap (due to Moss–Burstein shift) to the requisite 3.1 eV level [22,23].

6. Conclusions

The defect mechanisms observed in the $CdO\text{-}In_2O_3\text{-}SnO_2$ system can be divided into three categories—donor-doping mechanisms, ionic compensation mechanisms, and antisite disorder—as shown in Table 3. The first category, donor-doping, involves the production of shallow donor states, which effectively dope the conduction band with electrons (oxygen vacancies, cation substitutions with higher valence, and cation interstitials). Donor-doping can also be achieved by an inherent excess of donors (cations of higher valence)

than acceptors (cations of lower valence). The second category, ionic compensation, results in either a global balance of donors and acceptors (e.g. in the nominally 'stoichiometric' co-substituted solid solutions, and in oxygen vacancy-compensated acceptor-doping of the end-members) or a local balance of donors and acceptors (e.g. in the Sn-oxygen interstitial associate in ITO, which is electrically neutral). The co-substitution mechanism is significant, in that it permits wide ranges of solubility (the long 'vertical' solid solution lines in Fig. 1) and associated changes in important properties (e.g. band gap). The local (associate) mechanism is important in ITO, since it engenders enhanced Sn-solubility, and a subsequent reduction step can remove the oxygen interstitials and 'activate' the Sn donors. Finally, antisite disorder, which is unique to the spinel structure with its tetrahedral and octahedral cation sites, may play an important role governing phase stability and also the band structure. In particular, thermal history and/or solid solution composition can be employed to alter the fundamental gap in the spinel solid solution.

Acknowledgments

This work was supported by the MRSEC program of the National Science Foundation (grant no. DMR-0076097) through the Materials Research Center located at Northwestern University and the Department of Energy (grant no. DE-FG02-84ER45097) through the National Renewable Energy Lab under subcontract AAD-9-18668-05. DRK acknowledges the support of an NSF graduate fellowship and BJI acknowledges the support of a NDSEG fellowship.

References

[1] T.J. Coutts, T.O. Mason, J.D. Perkins, D.S. Ginley, in: V.K. Kapur, R.D. McConnell, D. Carlson, G.P. Ceasar, A. Rohtagi (Eds.), Photovoltaics for the 21st Century, PV99-11, Electrochemical Society, Pennington, NJ, 1999, p. 274.
[2] D.R. Kammler, B.J. Harder, N.W. Hrabe, N.M. McDonald, G.B. Gonzalez, D.A. Penak, T.O. Mason, J. Am. Ceram. Soc. (in press).
[3] D.R. Kammler, Ph.D. Thesis, Northwestern University, Evanston, IL, 2001.
[4] D.D. Edwards, T.O. Mason, J. Am. Ceram. Soc. 81 (1998) 3285.
[5] J.L. Bates, C.W. Griffin, D.D. Marchant, J.E. Garnier, Bull. Am. Ceram. Soc. 65 (1986) 673.
[6] L.V. Morozova, A.V. Komarov, Russ. J. Inorg. Chem. 36 (1991) 136.
[7] A.J. Smith, Acta Cryst. 13 (1960) 749.
[8] A.J. Nozik, Phys. Rev. B 6 (1972) 453.
[9] G. Haacke, W.E. Mealmaker, L.A. Siegel, Thin Solid Films 55 (1978) 67.
[10] X. Wu, T.J. Coutts, W.P. Mulligan, J. Vac. Sci. Technol. A 15 (1997) 1057.
[11] S. Choi, Y.H. Kang, K.H. Kim, J. Phys. Chem. 81 (1977) 2208.
[12] M.E. Straumanis, P.M. Vora, G. Lewis, A.A. Khan, Trans. Missouri Acad. Sci. 6 (1972) 92.
[13] H.J. van Daal, Solid State Commun. 6 (1968) 5.
[14] S. Sampson, C.G. Fonstadt, J. Appl. Phys. 42 (1971) 2911; 44 (1973) 4618.
[15] J. Maier, W. Göpel, J. Solid State Chem. 72 (1988) 293.
[16] E.C. Subbarao, P.H. Sutter, J. Hrizo, J. Am. Ceram. Soc. 48 (1965) 443.
[17] J.H.W. de Witt, J. Solid State Chem., 8 (1973) 142; 13 (1975) 192; 20 (1977) 143.
[18] J.H.W. de Witt, G. van Unen, M. Lahey, J. Phys. Chem. Solids 38 (1977) 819.
[19] E. Gartstein, T.O. Mason, J.B. Cohen, J. Phys. Chem. Solids 47 (1986) 759; 47 (1986) 775.
[20] F.M. Smits, Bell Syst. Tech. J. 37 (1958) 711.
[21] D.R. KammIer, T.O. Mason, K.R. Poeppelmeier, J. Am. Ceram. Soc. 84 (2001) 1004.
[22] H. Enoki, J. Echigoya, H. Suto, J. Mater. Sci. 26 (1991) 4110.
[23] G. Frank, H. Kostlin, Appl. Phys. A 27 (1982) 197.
[24] A. Wang, J.R. Babcock, N.L. Edleman, A.W. Metz, M.A. Lane, R. Asahi, V.P Dravid, C.R. Kannewurf, A.J. Freeman, T.J. Marks, Proc. Nat. Acad. Sci. 98 (2001) 7113.
[25] M. Yan, M. Lane, C.R. Kannewurf, R.P.H. Chang, Appl. Phys. Lett. 78 (2001) 2342.
[26] J.-H. Hwang, D.D. Edwards, D.R. Kammler, T.O. Mason, Solid State Ionics 129 (2000) 135.
[27] G.B. Gonzalez, J.B. Cohen, J.-H. Hwang, T.O. Mason, J. Appl. Phys. 89 (2001) 2550.
[28] R.D. Shannon, C.T. Prewitt, Acta Cryst. B 25 (1969) 925.
[29] D.R. Kammler, T. O. Mason, D.L. Young, T.J. Coutts, J. Appl. Phys. 90 (2001) 3263.
[30] W.P. Mulligan, Ph.D. Thesis, Colorado School of Mines, Golden, CO, 1997.
[31] S.-H. Wei, S.B. Zhang, Atomic chemical Potential Dependence of the Structural and Doping Properties of Cadmium Stannate (Cd_2SnO_4). Presented at the TMS 2000 Electronic Materials Conference, Denver, CO, 2000.
[32] L.N. Brewer, D.R. Kammler, T.O. Mason, V.P. Dravid, J. Appl. Phys. 89 (2001) 951.
[33] D. Ko, K.R. Poeppelmeier, D.R. Kammer, G.B. Gonzalez, T.O. Mason, D.L. Williamson, D.L. Young, T.J. Coutts, J. Solid State Chem., In Press.
[34] H.S.C. O'Neill, A. Navrotsky, Amer. Mineralogist 68 (1983) 181.
[35] T. Stapinski, E. Sapa, J. Zukrowski, Phys. Stat. Sol. A 103 (1987) K93.
[36] S.-H. Wei, S.B. Zhang, Phys. Rev. B 63 (2001) 45112.
[37] D.S. Ginley, C. Bright, Mat. Res. Soc. Bull. 25 (2000) 15.
[38] D.D. Edwards. Phase Relations, Crystal Structures, and Electrical Properties of Select Oxides in the Gallium-Indium-Tin-Oxide System. Ph.D. Thesis, Northwestern University, Evanston, IL, 1997.
[39] R.B.H. Tahar, T. Ban, Y. Ohya, Y. Takahashi, J. Appl. Phys. 83 (1998) 2631.